Preparation of Intercalated Mg-Al Layered Double Hydroxides and Its Application in PVC Thermal Stability

Xiaofei Zhang,[1,2,3] Tiaobao Zhao,[1,2] Hong Pi,[1,2] Shaoyun Guo[1,2]

[1]The State Key Laboratory of Polymer Materials Engineering, Sichuan University, Chengdu 610065, China
[2]Polymer Research Institute, Sichuan University, Chengdu 610065, China
[3]National Center for Packaging Material Quality Supervision and Inspection, Chengdu Institute of Product Quality Supervision and Inspection, Chengdu 610041, China

ABSTRACT: The Mg-Al oxide precursor prepared by the calcination of Mg-Al-carbonated layered double hydroxide (LDH) at 500 K for 4 h is used as the host material, 2-hydroxy-4-methoxybenzophenone-5-sulfonic acid (BP) is used as the guest material, BP-intercalated LDH (LDH-BP) is prepared by ion-exchange method. The structure of LDH-BP is characterized by X-ray diffraction (XRD), Fourier transform infrared (FTIR), and thermogravimetry and differential thermal analysis (TG-DTA). The thermal stability of PVC/BP, PVC/LDH, PVC/LDH-BP composites, as well as pure PVC is investigated by conventional Congo Red test and dynamic thermal stability analysis in both the open and closed processing environments. According to XRD and FTIR, BP anions have been intercalated into interlayer galleries of LDH. TG-DTA results show that the layer-anionic interaction results in the improvement of the thermal stability of BP. Congo Red tests indicate that the addition of BP catalyzes the thermal degradation of PVC. A little amount of LDH (such as 1 phr) makes PVC more stable, but excessive addition accelerates the thermal degradation of PVC. The addition of LDH-BP markedly improves the static thermal stability of PVC. The results of dynamic thermal stability tests in both the open and closed processing environments are consistent with that of Congo Red tests. © 2011 Wiley Periodicals, Inc. J Appl Polym Sci 124: 5180–5186, 2012

Key words: poly(vinyl chloride); (PVC); composites; thermal properties

INTRODUCTION

The low production cost, good processability, easy modification, and excellent chemical and fire resistance make PVC materials a very attractive and most suitable plastic for a wide variety of applications.[1–5] However, PVC materials have poor thermal stability that results in severe discoloration and loss of mechanical properties when exposed to heat or shear during melt-processing and practical applications.[1,6] Therefore, the addition of thermal stabilizers, such as lead salts, metal soaps, and organo-tin compounds, is necessary to improve the thermal stability of PVC. A number of recent publications reveal that the introduction of various kinds of additives, such as metal, metal oxides, metal chloride, metal hydroxides, metal carboxylates, calcium carbonate, and clay materials, which have been regarded as a secondary stabilizer, can further reinforce the thermal stability of PVC.[7–11] Among these additives, layered double hydroxide (LDH), also known as anion-exchanging minerals, has attracted much attention in the recent search for efficient additives to enhance PVC thermal stability. The stabilization mechanism to PVC mainly results from the HCl absorption capacity of LDH.[12–16] The reaction between LDH and HCl occurs in a two-step process. First, the counterions between LDH layers tend to react with HCl gas. Second, LDH layers react with HCl, which results in the complete destruction of LDH structure and the formation of metal chlorides. The conclusion is that the HCl absorption capacity of LDH is determined by its interlay distance to some degree. In addition, it is reported that more addition of LDH facilitates dehydrochlorination of PVC.[17] To solve these limitations of LDH in PVC materials, structural modification of LDH is usually done.

The general formula of LDH can be represented by $(M^{2+}_{1-x}M^{3+}_x(OH)_2)_{layer}(A^{n-}_{x/n} \cdot mH_2O)_{interlayer}$, where M^{2+} and M^{3+} represent divalent and trivalent cations, respectively; A^{n-} is an exchangeable inorganic anion; x is equal to the molar ratio $(M^{3+}/(M^{2+} + M^{3+})$; m is the number of water molecules located in the interlayer region together with

the anions. The pronounced anion-exchange capacity of LDH toward inorganic and organic anions facilitates the structural modification of LDH.[18–24] For example, the interlayer arrangement of anionic surfactants (alkyl sulfate and dodecyl glycol ether sulfate ions) in LDH has been studied extensively.[25,26] After intercalation, the interlayer distance of LDH increases, which can enhance the capacity of LDH to react with HCl and retard the degradation of PVC effectively.

However, the thermal stability of PVC after addition of anion-intercalated LDH was hardly reported. Liu et al.[27] achieved PVC/LDH nanocomposites using organo-LDH with DS^- and stearate anions in the interlayer space, and found that both the PVC/LDH-DS and PVC/LDH-stearate exhibited obviously enhanced thermal stability and increase of dehydrochlorination time in Congo Red tests relative to the pure PVC resin and the PVC/LDH-NO_3. Bao et al.[28] prepared PVC/LDH composites by alkyl phosphonate intercalated LDH, and also found that the composites presented an enhanced thermal stability.

2-hydroxy-4-methoxybenzophenone-5-sulfonic acid (BP) is known as an excellence anionic light stabilizer. However, the low molecular weight of BP is easily lost from polymer matrix through evaporation, migration, and extraction. Based on the anion-exchange capacity of LDH with the light stabilizers involving anionic groups, a large number of different anionic light stabilizers that have the similar chemical structure with BP have been intercalated into LDH.[29] Results show that physical loss of light stabilizers has been markedly weakened. Based on the conclusions above-mentioned, it is encouraging for us to construct a composite based on LDH and BP for both improving the physical stability of BP and investigating the effect of anion-intercalated LDH on the thermal stability of PVC.

In this work, BP anion-intercalated LDH is prepared by the anion-exchange method and the structure is characterized by X-ray diffraction (XRD), Fourier transform infrared (FTIR), and thermogravimetry and differential thermal analysis (TG-DTA). The thermal stability of PVC/BP, PVC/LDH, PVC/LDH-BP composites, as well as pure PVC in the presence of lead thermal stabilizer is investigated by conventional Congo Red test, dynamic thermal stability analysis in both the open and closed processing environments.

EXPERIMENTAL

Materials

PVC (SG-8 with a number-average molecular weight of 5.0×10^4) was purchased from Jinlu Group. (Sichuan, China). Tribasic lead sulfate and dibasic
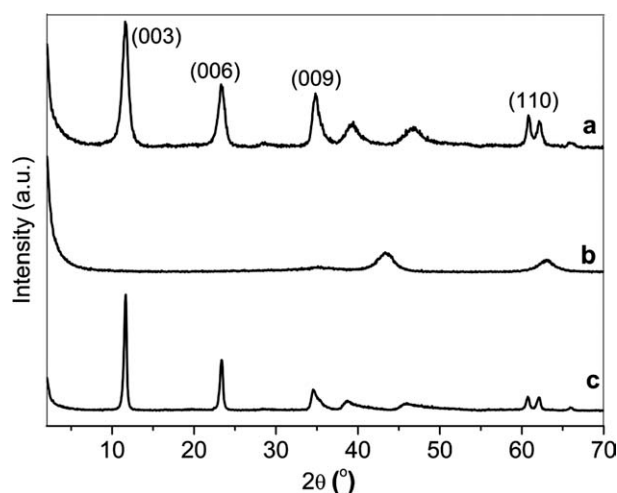

Figure 1 XRD patterns of (a) CO_3^{2-}/LDH, (b) LDO, and (c) OH/LDH.

lead phosphate were obtained from Tianshen Plastic Auxiliary Co. (Zhejiang, China). Stearic acid was purchased from Kelong Chemical Reagent Plant (Sichuan, China). Layered double hydroxide (CO_3/LDH) with Mg/Al = 2 : 1 was supplied by Fumeida New Materials Co. (Dalian, China). 2-Hydroxy-4-methoxy-benzophenone-5-sulfonic acid (BP) was obtained from B and S Group (Hongkong, China).

Preparation of intercalated Mg-Al layered double hydroxides

BP anion-intercalated LDH (BP-LDH) was prepared by anion-exchange reaction. Direct ion exchange is difficult as the carbonate in the interlayer galleries of LDH (CO_3/LDH) is held tenaciously. The LDH was modified by regeneration method, which is based on the well-known "memory effect." The Mg-Al oxide precursor used for the intercalation reaction of BP was obtained by the calcinations of the CO_3/LDH at 500°C in a muffle furnace for 4 h and the calcined LDH is called LDO. Figure 1 shows the XRD patterns of CO_3/LDH, LDO, and LDH after calcination-rehydration reaction (OH/LDH). The main diffraction peaks of the CO_3/LDH ($d_{003} = 0.76$ and $d_{006} = 0.38$ nm) were observed in Figure 1(a), in which the values are in good agreement with that of the synthetic hydrotalcite-like compound and the crystallite size of the CO_3/LDH is 33.2 nm. The destruction of the CO_3/LDH structure was achieved by heating at 500°C for 4 h, which can be seen by the disappearance of (003) and (006) reflections and the appearance of broad peaks of MgO in Figure 1(b). As a reference, OH/LDH was observed to have the LDH structure ($d_{003} = 0.76$ and $d_{006} = 0.38$ nm) with the disappearance of MgO reflection when the Mg-Al oxide precursor was rehydrated in distilled water (noncontaining BP) in Figure 1(c), meaning that the

Mg-Al oxide precursor regenerated the LDH structure (OH/LDH) by the rehydration reaction.

A 200-cm^3 three-necked round-bottom flask equipped with reflux condenser, thermometer, mechanical stirrer, and electric heating mantle was charged with 100 cm^3 of boiled water and 4.0 g of BP. After well dissolving, 8.0 g of LDO powder was dispersed in aqueous solution. The suspension was kept at 100°C for 48 h with vigorous stirring under a nitrogen atmosphere to prevent the formation of the CO$_3$/LDH. The product was filtered out, washed with boiled distilled water several times to remove excess adsorbed BP, and dried at 50°C for 24 h.

Sample preparation

Hundred parts of PVC, tribasic lead sulfate (powder, 2 phr), dibasic lead phosphite (powder, 1 phr), stearic acid (powder, 0.5 phr), and LDH or LDH-BP were dry-blended. The mixture was milled by an open twin-roller at 180°C for 5 min. Then, the PVC sheet was stirred into powder for the Congo Red testing. The composition of samples for dynamic thermal stability analysis was the same with that of the Congo Red testing.

Measurements and characterization

Powder XRD measurements were performed on a Shimadzu XRD-6000 X-ray powder diffractometer (Cu Ka radiation, 40 kV, 100 mA) between 2 and 70°. The scan speed was 6°/min.

The infrared spectra of samples were obtained by using a Nicolet 560 FTIR Spectrometer. Approximately 1.0 mg sample added with ∼ 200 mg dried KBr was ground in an agate bowl, and pressed into a transparent slice by a ∼ 400 kg/cm^2 pressure for about 2 min. Forty scans were acquired at a resolution of 1 cm^{-1}.

TG-DTA curves were obtained on Q50 (TA instrument) in the temperature range of 50–700°C with a heating rate of 10°C/min in a N$_2$ flow.

Particle size distribution of suspended particles in water was conducted by Malvern Mastersizer 2000 particle size analyzer (Worcestershire, UK).

The Congo Red test was carried out according to the standard of ASTM D4202. Glycerol was used as oil bath. The test temperature was 180°C. This method was also called the "static thermal stability analysis."

For dynamic thermal stability analysis in the open processing environment, PVC/thermal stabilizers mixture was milled in an open twin-roller at 170°C. The mixture was milled till its color turned purple. The dynamic thermal stabilizing time is defined as the time when its color starts to turn purple.
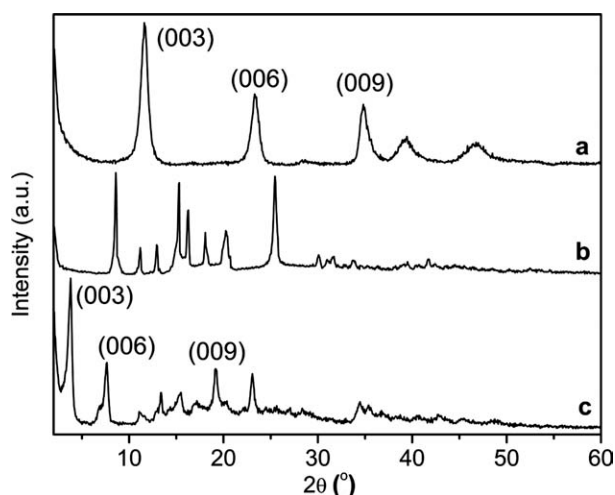
Figure 2 XRD patterns of (a) LDH, (b) BP, and (c) LDH-BP.

For dynamic thermal stability analysis in the closed processing environment, PVC/thermal stabilizer mixture was tested in the mixing chamber of a Haake Rheometer RC90 at 185°C and a rotor speed of 30 rpm. The dynamic thermal stabilizing time is defined as the time when the color starts to turn purple.

RESULTS AND DISCUSSION

Characterization of intercalated Mg-Al layered double hydroxides

XRD analysis

The XRD patterns of LDH, BP, and LDH-BP are shown in Figure 2. The XRD pattern of LDH [Fig. 2(a)] exhibits the characteristic pattern of a layered solid with sharp, symmetrical peaks at low angle corresponding to the basal reflection and higher order reflections, and some asymmetrical peaks at high angle. The (003), (006), and (009) diffraction peaks appear at 11.6, 23.3, and 34.8°, respectively. The basal spacing (d_{003}) of the LDH is 0.76 nm. The diffraction peaks in Figure 2(b) indicate the typical structure of BP. After BP anions are intercalated into the interlayer galleries of LDH, the reflections (003), (006), and (009) have been noticed at lower angles with an increase in the basal spacing as shown in Figure 2(c). The new (003), (006), and (009) diffraction peaks move to 3.79, 7.63, and 11.47°, respectively. The interlayer distance of (003) peak increases from 0.76 nm in the case of LDH to 2.33 nm for LDH-BP, indicating that BP anions have replaced CO_3^{2-} in the interlayer galleries to form LDH-BP. The (009) reflection of the intercalated samples seems to be (003) of LDH before intercalation, but from the X-ray calculations the peak locates at $2\theta = 11.47°$ with an interlayer distance 0.77 nm. The

TABLE I
Indexing of XRD Patterns for LDH and LDH-BP

Parameter (nm)	LDH	LDH-BP
d_{003}	0.76	2.33
d_{006}	0.38	1.16
d_{009}	0.26	0.77
d_{110}	0.15	0.15
Lattice parameter a	0.30	0.30
Lattice parameter c	2.28	6.99

strong sharp reflections indicate that the LDH-BP have a well-formed crystalline-layered structure.

Indexing of XRD patterns for LDH and LDH-BP is shown in Table I. According to bond-length and bond-angle data, the length of the BP anion calculated is 1.16 nm. The XRD data indicate that the interlayer distance of LDH/BP is 2.33 nm. Subtracting the thickness of the LDH layer (0.48 nm), the gallery height of LDH/BP is 1.85 nm, which is much larger than that of the ion size.[30,31] Xu and Zeng[32] have demonstrated that the value of the basal spacing for nitrate-containing LDH is very sensitive to the NO_3^- content that is a function of the Mg^{2+}/ Al^{3+} ratio. Values of $d_{003} < 0.82$ nm are associated with low nitrate content, and in such materials the nitrate anions lie in the center of the interlayer galleries. Values of $d_{003} > 0.82$ nm are characteristic of high nitrate content, and it has been suggested that nitrate anions are alternatively associated with upper and lower metal hydroxide layers to relieve steric rowding. Therefore, it was suspected that, just as the latter of NO_3^-, BP anions located in a line by turning the functional group on the contrary by turns and linked to the upper and lower layers. The excessive space between the BP anions is occupied by water molecules as shown in Figure 3.

FTIR analysis

FTIR spectra of LDH, BP, and LDH-BP are shown in Figure 4. A broad absorption peak in the 2800–3600 cm^{-1} region is assigned to O—H group stretching and deformation vibration of the hydroxide basal layer or interlayer water molecules. The strong peak at 1366 cm^{-1} is attributed to the stretching mode of CO_3^{2-}. In curve b of Figure 4, the strong absorption bands at 1274, 1082, and 1022 cm^{-1} are attributed to the typical peaks of SO_3^{2-} groups of BP. After intercalation, the absorption band of CO_3^{2-} groups disappeared as a result of the replacement of CO_3^{2-} groups by BP anions. The band at 1274, 1082, and 1022 cm^{-1} in BP shifted to a higher frequency and located at 1278, 1087, and 1029 cm^{-1} as shown in curve c. This can be ascribed to the strong hydrogen bonding interactions between the sulfonate groups and adjacent hydroxyl groups of the layers.
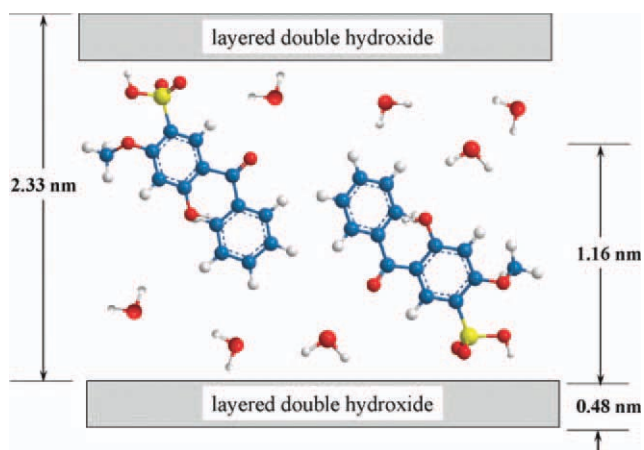

Figure 3 Schematic representation of LDH-BP. [Color figure can be viewed in the online issue, which is available at wileyonlinelibrary.com]

TG-DTA analysis

Figure 5 shows the TG-DTA curves of LDH, BP, and LDH-BP. The DTA curve of LDH [Fig. 5(a)] has an endothermic peak near 101°C with a corresponding weight loss in the TG curve. This is attributed to the loss of the physically absorbed water on the LDH molecules.[33] With increasing temperature, there is a weight-loss stage in the range of 200–300°C in the TG curve. The weight loss in this range can be attributed to the desorption of interlayer water between LDH molecules. After 300°C, a sharp weight-loss process appears. This weight loss process can be attributed to the dehydroxylation and the decomposition of carbonate ions of the LDH. The formation of MgO and $MgAl_2O_4$ has been observed in the TGA residue by XRD, which is in agreement with a previous result.[33]
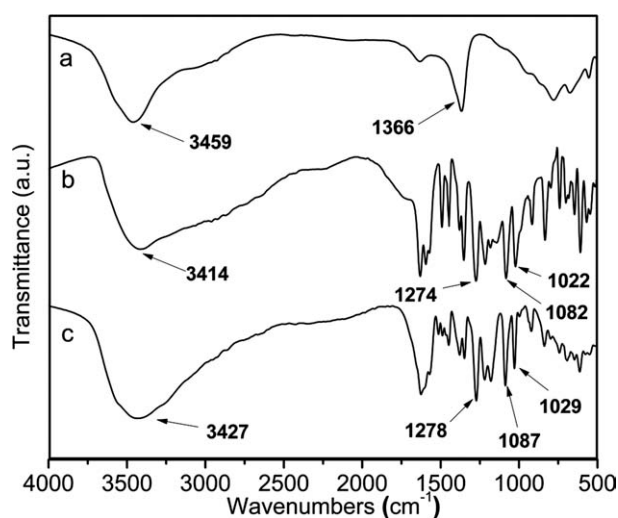

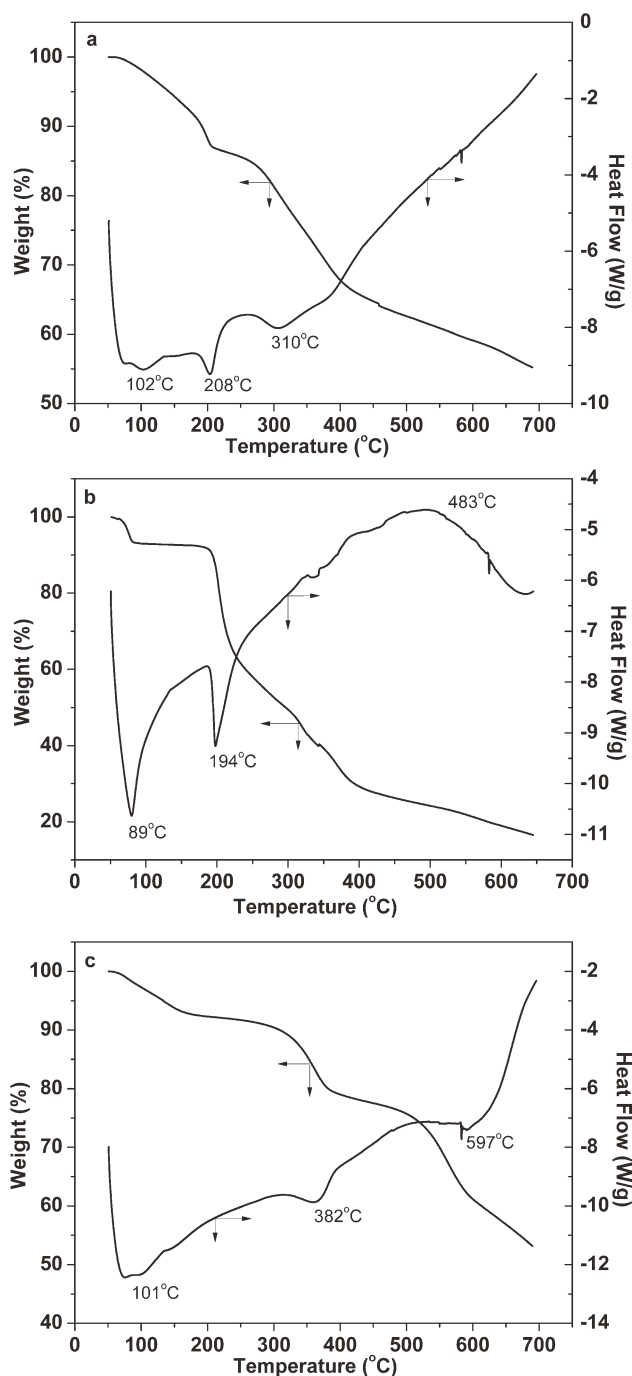Figure 4 FTIR spectra of (a) LDH, (b) BP, and (c) LDH-BP.

Figure 5 TG-DTA curves of (a) LDH, (b) BP, and (c) LDH-BP.

Figure 5(b) shows the TG-DTA curves of BP. The endothermic peak at 89°C in the DTA curve corresponds to the melt point of BP. The strong exothermic peak at 194°C can be assigned to the decomposition of BP. This is why physical loss of BP happens easily. The exothermic peak near 483°C can be attributed to the combustion of BP anion fragments. All the three processes have their corresponding weight-loss stages in the TG curve.

After the intercalation of the BP anions into the LDH host, the thermal decomposition behavior of

the resulting product is significantly different from that of the LDH. The thermal degradation of the LDH-BP takes place in several steps. As shown in Figure 5(c), the first step is attributed to loss of absorbed water. The endothermic peak noted at 101°C in the DTA curve corresponds to the absorbed water. Liberation of adsorbed water from the interlayer galleries of the intercalate results in an endothermic peak at 382°C with a corresponding weight loss between 300 and 400°C in the TG curve, ∼ 70°C higher than the corresponding peak for the LDH. As mentioned in the XRD analysis, the amount of water in LDH-BP is significantly higher than that in the LDH due to the larger space available in the expanded interlayer galleries. These two phenomena indicate that the water is more strongly bound in the interlayer galleries after intercalation of the BP anions. The strong endothermic band at 597°C is due to the decomposition of the organic guest. It can be concluded from TG-DTA analysis that the thermal stability of BP has been enhanced after intercalation to some extent. This is consistent with the presence of a strongly hydrogen-bonded network in the interlayer galleries involving the hydroxyl groups of the layers, the anionic ions in BP, as well as interlayer water molecules.

The TG-DTA data indicate that LDH-BP is a complex system of strong supramolecular interactions between LDH layers and BP anions. The interactions involve electrostatic attraction between opposite charges and hydrogen bonding. It is the layer-anion interaction that results in the improvement of the thermal stability of BP.

Thermal stability

Static thermal stability

The Congo Red test is a measure of the remaining capacity of the stabilizing samples. In thermostabilizer-doped PVC, if PVC is degraded, the liberated HCl reacts with the stabilizer, and a long static thermal stability time is observed. Through measuring the concentration of the HCl, one can qualitatively analyze the static thermal stability of PVC materials.

Figure 6 shows the influences of LDH, BP, and LDH-BP on the static thermal stability and the dehydrochlorination process of PVC measured by the Congo Red tests. What should be mentioned is that the samples for static thermal stability were first milled by an open twin-roller at 180°C for 5 min. The static thermal stability time of the samples that degraded during milling was not recorded. The static thermal stability time of the pure PVC is only about 97 min. After the addition of BP, the time drops below 50°C. Because of the sulfonic acid group in BP structure, the pH value of BP is less
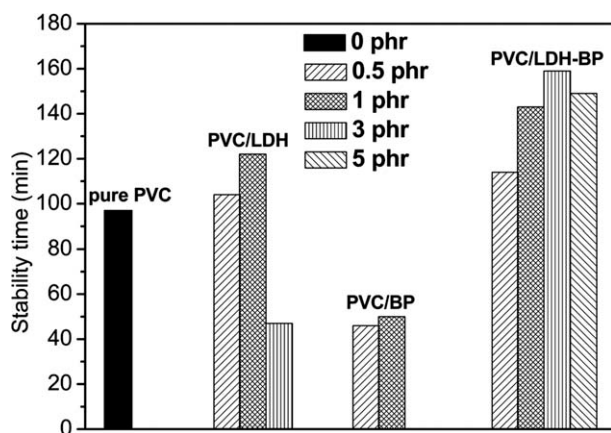
Figure 6 Thermal stability time of PVC, PVC/LDH, PVC/BP, and PVC/LDH-BP measured by Congo Red test.

than 2 and the strong acid catalyzes the thermal degradation of PVC.

LDH can prolong the degradation of PVC and improve the color stability due to absorption of HCl when used in combination with other main thermal stabilizers. In this experiment, the addition of 0.5 or 1.0 phr of LDH enhances the static thermal stability of PVC, and the stability time is 105 and 120°C, respectively. However, further addition of LDH, such as 3.0 phr, accelerates the degradation of PVC and the stability time decreases below 50°C. LDH can absorb HCl gas liberated from the dehydrochlorination reaction of PVC, retard the degradation process of PVC in ionic mechanism, and improve the thermal stability of PVC. However, excessive addition of LDH triggers the degradation of PVC due to the alkalescency of LDH that cannot be neutralized by HCl.

Being different with the thermal behavior of PVC after the addition of BP or LDH, the stability time continues increasing with the addition of LDH-BP. After adding 0.5 phr of LDH-BP, the stability time of PVC extends to 110°C. For 3 phr of LDH-BP, this value raises up to 160°C, which is over 1.6 times of that of the pure PVC and longer than that of PVC/LDH composite. This result indicates that the addition of LDH-BP facilitates the HCl absorption during the dehydrochlorination process of PVC.

The absorption of HCl by LDH can be explained in the following:

1. HCl reacts with the LDH layers, following the complete destruction of the LDH structure and formation of metal chlorides.
2. After the intercalation of BP into LDH, the interlayer distance increases from 0.76 to 2.33 nm, and facilitates both the entry of Cl^- into the interlayer galleries and the reaction between HCl and the layers.

3. Because of the intercalation, the acid and alkali catalysis of LDH-BP disappear, and the excessive additive of LDH-BP further enhances the stability of PVC.

Thermal processing stability

Except high temperature, PVC endures strong shear force during thermal process. Because of the existence of shear force, the stability of PVC deteriorates in the thermal processing stability as shown in Table II. The sulfonic acid of BP can catalyze the degradation of PVC, just as the behavior in the static thermal stability experiment and the existence of shear force accelerates this behavior. Being similar to the results of static thermal stability experiment, the result of dynamic thermal stability in the open processing environment shows that a little amount of LDH (such as 0.5 phr) makes PVC more stable, while excessive addition accelerates the thermal degradation of PVC. However, the addition of LDH-BP markedly improves the static thermal stability of PVC. The improvement of the thermal stability of PVC/LDH-BP composites is attributed to the good dispersed LDH-BP and the elimination of the alkali of LDH after intercalation as well as the strong HCl absorption capacity of LDH-BP. On one hand, LDH-BP particles are homogeneously dispersed in PVC matrix, resulting in enormous interface area and strong interfacial interaction between PVC and LDH-BP. The particle size distribution of LDH and LDH-BP in Figure 7 verifies this result. Good dispersion can weaken the friction between LDH-BP and PVC. In addition, good dispersion has obvious effect on the absorption

TABLE II
Effect of Different Processing Methods on the Thermal Stability of PVC

Compound	Additive content (phr)	Time to degradation (min)	
		Processing on a two-rolling mill (180°C)	Processing on a HAAKE (185°C, 30 r/min)
Pure PVC		20	11
PVC/BP	0.5	15	9
	1	12	4
	3	a	a
	5	a	a
PVC/LDH	0.5	25	13
	1	18	8
	3	8	a
	5	a	a
PVC/LDH-BP	0.5	≥30	15
	1	≥30	13
	3	≥30	12
	5	≥30	13

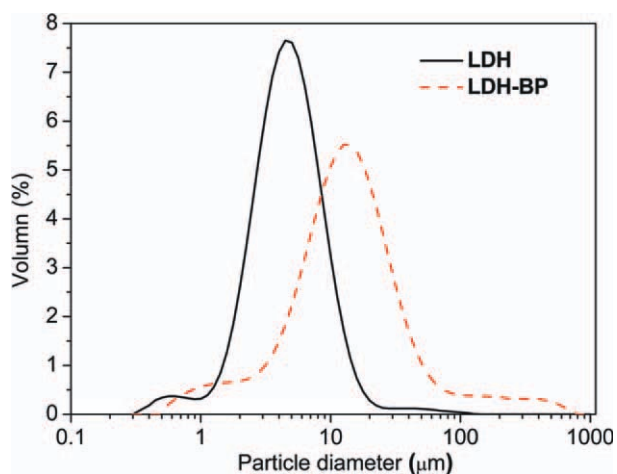ᵃThe samples degraded during milling.

Figure 7 Particle size distribution of LDH and LDH-BP. [Color figure can be viewed in the online issue, which is available at wileyonlinelibrary.com]

capacity to the liberated HCl. On the other hand, after the intercalation of BP anions into LDH, the neutralization reaction occurs. Both the acidity of BP and the alkali of LDH disappear and cannot catalyze the thermal degradation of PVC. Furthermore, the stabilizing effect of PVC and PVC composites was also observed by the HAAKE Rheometer RC90. Similar results are obtained in Table II.

CONCLUSIONS

BP has been intercalated into a LDH by ion-exchange method in water, and the interlayer distance after intercalation increases from 0.76 to 2.33 nm. The thermal stability of BP is significantly enhanced due to strong supramolecular interactions between LDH layers and BP anions.

Congo Red tests show that the addition of BP catalyzes the thermal degradation of PVC, because of its acid properties. HCl absorption capacity of LDH makes PVC more stable, but the alkalescence of LDH accelerates the degradation of PVC after excessive addition. The acid and alkali catalysis of LDH-BP disappear after intercalation, and the interlayer distance of LDH increases from 0.76 to 2.33 nm, which facilitates the reaction between HCl and the layers. The excessive addition of LDH-BP can markedly improve the static thermal stability time of PVC.

The results of the dynamic thermal stability analysis in both the open and closed processing environments are similar to those of static thermal stability. In addition, due to the existence of shear force, PVC degrades more quickly in the dynamic thermal stability experiment. The better dispersion of LDH-BP results in higher exposure of the PVC matrix to the LDH-BP, weakens the friction between LDH-BP and

PVC, has obvious effect on the absorption capacity of the released HCl, and eventually increases the thermal stability of PVC.

References

1. Owen, E. D. Degradation and Stabilization of PVC; Elsevier Applied Science Publishers: New York, 1984.
2. Kaczmarek, H.; Kowalonek, J.; Oldak, D. Polym Degrad Stab 2003, 79, 231.
3. Kaczmarek, H.; Swiatek, M.; Kaminska, A. Polym Degrad Stab 2004, 83, 35.
4. Gesenhues, U. Polym Degrad Stab 2000, 68, 185.
5. Jakubowicz, I. Polym Test 2001, 20, 545.
6. Rabek, J. F. Polymer Photodegradation—Mechanisms and Experimental Methods; Chapman & Hall: London, 1995.
7. Benbaniba, M. T.; Benlhaneche-Bensemra, N.; Gelbard, G. Polym Degrad Stab 2001, 74, 501.
8. Miyata, S.; Nosu, T. Eur. Pat. Appl. 0256872, 1988.
9. Sevdiye, A.; Devrim, B.; Semra, U. J Vinyl Addit Technol 2005, 11, 47.
10. Razvan, C.; Beck, R.; Kurzinger, A.; Purzer, A. W.; Rosenthal, M. Ger. Pat. Spec. DE 3941902 Cl, 1991.
11. Wang, M.; Xu, J. Y.; Wu, H.; Guo, S. Y. Polym Degrad Stab 2006, 91, 2101.
12. Zhang, Q.; Li, H. Spectrochim Acta A Mol Biomol Spectrosc 2008, 69, 62.
13. Liu, J.; Chen, G. M.; Yang, J. P. Polymer 2008, 49, 3923.
14. Gu, Z.; Liu, W. S.; Dou, W.; Tang, F. Polym Compos 2010, 31, 928.
15. Liu, J.; Chen, G. M.; Yang, J. P.; Ding, L. P. J Appl Polym Sci 2010, 116, 2058.
16. Van Der Ven, L.; Van Gemert, M. L. M.; Batenburg, L. F.; Keern, J. J.; Gielgens, L. H.; Koster, T. P. M. Appl Clay Sci 2000, 17, 25.
17. Xu, Z. P.; Saha, S. K.; Braterman, P. S.; D'Souza, N. Polym Degrad Stab 2006, 91, 3237.
18. Boehm, H. P.; Steinle, L.; Viewen, C. A. Angew Chem Int Ed Engl 1977, 89, 259.
19. Dutta, P. K.; Puri, M. J Phys Chem 1989, 93, 376.
20. Mendibourc, A.; Schdllhorn, R. Revue Chimie Miner 1986, 23, 819.
21. Sasaki, M.; Mikani, N.; Ikeda, T.; Hachiya, K.; Yasunaga, T. J Phys Chem 1982, 86, 4413.
22. Giannelis, E. P.; Nocera, D. G.; Pinnavaia, T. J Inorg Chem 1987, 29, 163.
23. Mikami, N.; Sasaki, M.; Horibe, S.; Yasunaga, T. J Phys Chem 1984, 88, 1716.
24. Suzuki, E.; Idemura, S.; Ono, Y. Clays Clay Miner 1989, 37, 173.
25. Miyata, S.; Kumura, T. Chem Lett 1973, 23, 843.
26. Kopka, H.; Beneke, K.; Lagaly, G. J Colloid Interface Sci 1988, 123, 427.
27. Liu, J.; Chen, G.; Yang, J.; Ding, L. Mater Chem Phys 2009, 118, 405.
28. Bao, Y. Z.; Huang, Z. M.; Weng, Z. X. J Appl Polym Sci 2006, 102, 1471.
29. Lin, Y. J.; Wang, J. R.; Evans, D. G.; Li, D. Q. J Phys Chem Solids 2006, 67, 998.
30. Choy, J. H.; Kwar, S. Y.; Jeong, Y. J.; Park, J. S. Angew Chem Int Ed Engl 2000, 39, 4042.
31. He, Q.; Yin, S.; Sato, T. J Phys Chem Solids 2004, 65, 395.
32. Xu, Z. P.; Zeng, H. C. J Phys Chem B 2001, 105, 1743.
33. Newman, S. P.; Jones, W. New J Chem 1998, 22, 105.